# Numerical Simulation for Strength and Stability of RC Tapered Columns

**Jabbar Abdalaali Kadhim**
Department of Civil Engineering, College of Engineering, University of Baghdad, Iraq
jabaralkhafaji1981@gmail.com (corresponding author)

**Salah R. Al-Zaidee**
Department of Civil Engineering, College of Engineering, University of Baghdad, Iraq
salah.r.al.zaidee@coeng.uobaghdad.edu.iq

*Received: 10 March 2024 | Revised: 18 April 2024 | Accepted: 3 May 2024*



## ABSTRACT

**This study investigates the strength and stability of Reinforced Concrete (RC) linearly tapered square columns. Evaluating the slenderness ratio of an RC column requires the radius of gyration of its cross-section, which is well-defined for a prismatic column but not for a non-prismatic one. This study primarily investigates the application of the ACI Code formulae to evaluate the slenderness ratio of RC columns with the studied geometry. Validated numerical models, using Abaqus, were employed to perform nonlinear first- and second-order analyses on the investigated columns subjected to eccentric axial loads. The concrete damaged plasticity model was employed to simulate the nonlinear behavior of concrete. The static Riks solver, available in Abaqus, was utilized for nonlinear analyses: first, with an inactivated geometric nonlinearity for a first-order analysis, and second, with an activated geometric nonlinearity to consider the effects of secondary moments ($p$-$\delta$ effects). The findings indicate the reliability of defining the slenderness ratio of an RC linearly tapered column based on the ACI Code formulae, using the average cross-section of the tapered column.**

***Keywords-reinforced concrete; non-prismatic columns; slenderness ratio; secondary moment; Abaqus***

## I. INTRODUCTION

RC non-prismatic columns appear in civil structures to satisfy structural and/or architectural goals [1]. As the axial loads in columns decrease in multi-story buildings from top to bottom, columns that are tapered from larger cross-sections at the bottom to smaller cross-sections at the top optimize the structural design. Large cross-sections in the lower stories increase the strength where the axial loads, shear forces due to lateral loads, and overturning moments are higher than those in the upper stories. In addition, the weight of the structure is reduced compared to the construction of columns with constant cross-sections along the height of the building [2]. In addition, they are used on highway bridges to reduce the moment transferred to the foundation [3]. Such columns are still not covered by the codes for stability and other design limitations. Some studies dealt with the elastic and inelastic stability of homogeneous non-prismatic columns, whereas few studies focused on RC non-prismatic columns. The structural behavior of reinforced concrete has its distinct nature due to the interaction between the steel and the surrounding concrete. The propagation of microcracks results in a high nonlinearity in the structural response of concrete [4].

In [5], the behavior of slender, hinged-hinged, tapered RC columns was theoretically and experimentally investigated under the effect of eccentric loads. The experimental program involved testing 19 full-scale columns. The study adopted the average cross-section to evaluate the slenderness ratio. This study also introduced charts for the design of RC tapered columns, which are also applicable to prismatic ones. In [6], rational analysis was introduced to predict the maximum strength and structural response of slender RC columns that are linearly tapered under the effect of axial loading and end moments. The columns were doubly symmetric rectangular columns with main reinforcement parallel to the edges. This study revealed that as the ratio of the moment applied at the smaller end to that applied at the greater end approaches zero, the capacity of the axial load increases. This study showed that tapered columns become less efficient if the end moments are equal with single or double curvature bending and also when they are very small. This study recommended that the end cross-sections should be proportioned so that the ratio of their moments of inertia is the same as the ratio of end moments.

In [7], fabric formworks were deployed to study the strength of the columns of variable cross-sections, all having the same height and axial loads. The results revealed that the weaker column had a convex geometry and experienced sudden failure. This behavior is attributed to the transverse tensile stresses developed in the bulging columns, which cause longitudinal cracks and subsequent crushing of the column.

This case was inversed in concave columns. In [8], the structural behavior of hollow and solid non-prismatic RC columns was experimentally investigated. The results suggested that a 50% increase in longitudinal reinforcement raises the axial load capacity by 25%, whereas the same augmentation in transverse reinforcement increases the load capacity by 12%. In [3], the buckling of slender, square, tapered concrete columns, reinforced with longitudinal reinforcement parallel to the inclined edges of the columns, was investigated. Analytical and numerical Abaqus analyses on column models disclosed that a tapering ratio (slope of column longitudinal edges) greater than 150 does not affect the buckling load and is just an aesthetic feature.

None of these studies investigated the relationship between the slenderness ratio of RC non-prismatic columns and the *p-δ* effect (effect of secondary moment), and whether the formulae of the ACI Code established for prismatic columns can be applied to non-prismatic columns. This study investigates the possibility of dealing with an RC non-prismatic column to evaluate its slenderness ratio as a prismatic column having a cross-section equal to its average cross-section. The numerical model can be validated by comparing it with experimental results, analytical models, or semi-empirical results as in [9]. The finite element modeling in Abaqus was validated in [10] by comparing numerical and experimental results. The nonlinear static Riks solver, which is suitable for nonlinear solutions, especially in the descending part of the load-deflection relationship, was used to perform the nonlinear analyses. First, this study compared the Abaqus results with the ACI Code limitations for the slenderness ratio of two prismatic columns. This comparison of the two prismatic models was performed as an additional validation for numerical modeling, which was already validated by comparing the numerical and experimental results. The concrete-damaged plasticity available in Abaqus was employed to simulate the nonlinear behavior of concrete. The parameters of this model were calibrated with many test results [11]. The column is considered short if the *p-δ* effect does not reduce its axial load capacity by more than 5%, otherwise it is long, which is the criterion adopted by the ACI Code [12]. Abaqus offers the choice between first- or second-order analysis. The first-order analysis means that the structure is analyzed based on its original undeformed shape, and thus the secondary moments caused by the loads and deformations are neglected. In other words, geometric nonlinearity is not considered. On the contrary, the second-order analysis is the analysis of the structure in which its equilibrium is based on the deformed shape [13-15]. This study performed both analyses for each model to evaluate the reduction in the axial load capacity due to the effects of secondary moments. For all models studied, the boundary conditions were chosen so that all were pin-ended. The top end of the column was free to move downward in the y-direction and both ends were free to rotate about the x-direction.

## II. MATERIAL STRENGTHS AND CONSTITUTIVE RELATIONSHIPS

For all models, the compressive strength of the concrete was 30 mPa and the yield stress of the steel reinforcement was 400 mPa. The parabolic constitutive model for concrete compressive behavior proposed in [16] was utilized. According to this model, the compressive stress in concrete is:

$$\sigma_c = f_c' \left[ 2\left(\varepsilon_c / \varepsilon_o\right)^2 - \left(\varepsilon_c / \varepsilon_o\right)^2 \right] \quad (1)$$

where $\sigma_c$ is the concrete compressive stress, $f_c'$ is the compressive strength of concrete, $\varepsilon_c$ is the concrete compressive strain, and $\varepsilon_o$ is the concrete compressive strain corresponding to the peak stress value. $\varepsilon_o$ was taken equal to 0.002. A linear relationship for the tensile behavior of concrete was deployed, which was taken equal to the modulus of rupture $0.62\sqrt{f_c'}$ , In both tension and compression, a bilinear elastic-full plastic model was implemented for steel reinforcement.

## III. PRISMATIC MODELS

### A. Model 1

Model 1 has a length of 1980 mm and a cross-section of 300×300 mm. The four longitudinal rebars had Ø 20 mm and the transverse reinforcement was Ø 10 mm at 200 mm. Figure 1(a) depicts the view cut numerical model. The top-end eccentricity is 25 mm, the same as that at the bottom end. Figure 1(b) illustrates the failure mode of the column. Figure 2 portrays the load-deflection relationships.

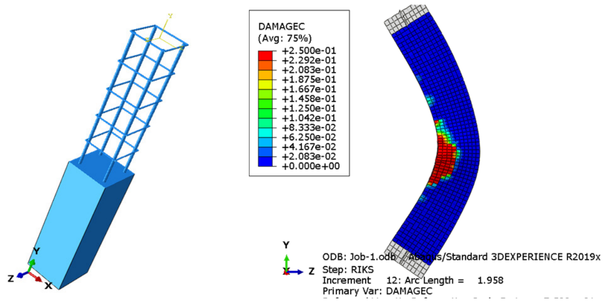


Fig. 1. Model 1: (a) view cut, (b) failure mode.

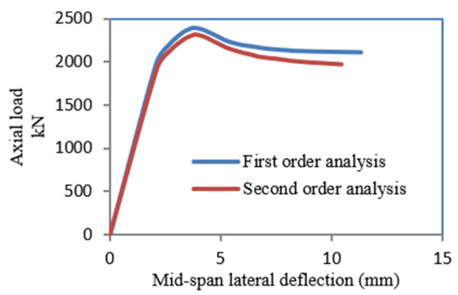


Fig. 2. Model 1 load-deflection relationships ($\rho$ = 0.014).

The results of the first- and second-order analyses for the load capacity were 2389.7 and 2317 kN, respectively. Thus, the reduction in axial load capacity caused by the secondary moment was 3%, which is less than 5%, the limit beyond which the ACI Code classifies a column as slender or long. For frames braced against side sway, the ACI Code [17] classifies an RC column as a short column if its slenderness ratio does not exceed the value given by:

$$\frac{k\,l_u}{r} \leq 34 + 12\frac{M_1}{M_2} \quad (2)$$

where $k$ is the effective length factor, $l_u$ is the unsupported length of the column, $r$ is the radius of gyration of the column cross-section, $M_1$ is the smaller end moment, and $M_2$ is the greater end moment. The value $M_1/M_2$ shall be negative if the end moments produce a single curvature. The slenderness ratio of Model 1 is evaluated as follows:

$$\frac{k\,l_u}{r} = \frac{1*1980}{0.3*300} = 22 \quad (3)$$

For a single curvature loading, as in the case of loading Model 1, the limiting value given by (2) is 22, which means that it is a short column but at the transition limit between short and long columns. If $M_1$ is zero, the limit given by (2) becomes 34, which is much greater than the slenderness ratio of Model 1. In this case, the column is short and far from the transition limit of the slenderness ratio. Therefore, the 3% reduction in load capacity given by the Abaqus analysis indicates that the effect of the secondary moment is still relatively far away from the criterion value of 5%. It can be interpreted that the ACI Code is conservative for the case of a single curvature since the lateral deflection is expected to be larger compared to the double curvature cases or when $M_1$ equals zero. However, the numerical simulation of Abaqus predicted well the slenderness effect of the model. The steel reinforcement ratio, the steel reinforcement area divided by the gross area of the cross-section, was changed from 0.014 to 0.0218, and the analysis was repeated for first- and second-order analysis. Ignoring the effect of the secondary moment, the Abaqus result for the load capacity was 2618.7 kN, whereas this became 2543 kN when taking into account geometric nonlinearity. Thus, the reduction in the axial load capacity was 2.88%. Figure 3 presents the load-deflection relationships for Model 1 after changing the reinforcement ratio.

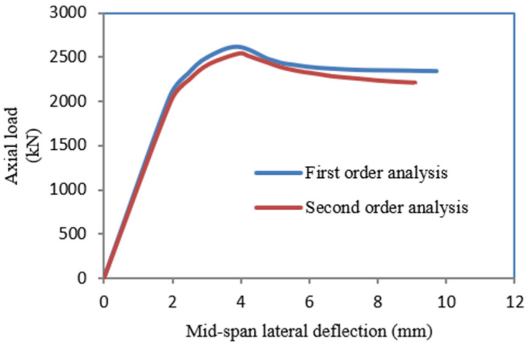


Fig. 3. Model 1 load-deflection relationships ($\rho$ = 0.0218).

It can be seen that increasing the steel reinforcement ratio reduces the effects of secondary moments. The higher the reinforcement ratio is, the less the *p-δ* effects are. This result agrees with the fact that increasing the steel reinforcement area in the concrete section augments the flexural rigidity of the column, which, in turn, increases its structural stiffness. Increasing the stiffness reduces the lateral deflection, and thus the *p-δ* effects are mitigated. The steel ratio of 0.014 is very close to the minimum reinforcement ratio required by the ACI Code for concrete columns, which is 0.01 [17]. Thus, the finite element analysis will give less secondary moment effects for any other higher reinforcement ratio. This agrees with the fact that the code adopts only the length and the dimensions of the cross-section of the column to evaluate its slenderness ratio regardless of the amount of steel reinforcement.

### *B. Model 2*

Model 2 has the same properties as Model 1 except for the length, which is 3600 mm. Conssequently, it is a slender column having a slenderness ratio of 40. The column model is pin-ended with 15 mm eccentricity at each end. The steel reinforcement ratio is 0.014. Figure 4 exhibits the failure mode of Model 2 and the stresses in steel reinforcement. Figure 5 displays the load-deflection relationships.

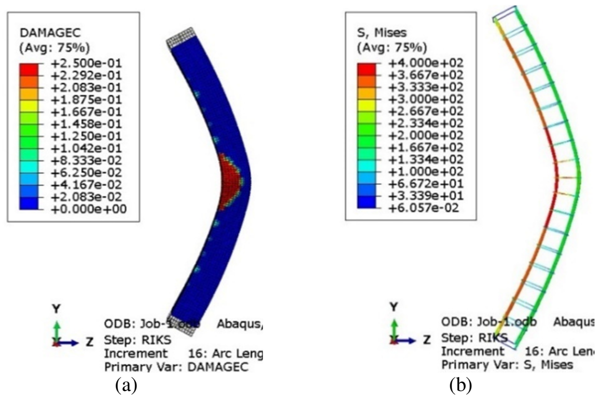


Fig. 4. Model 2: (a) failure mode (b) reinforcement stresses.

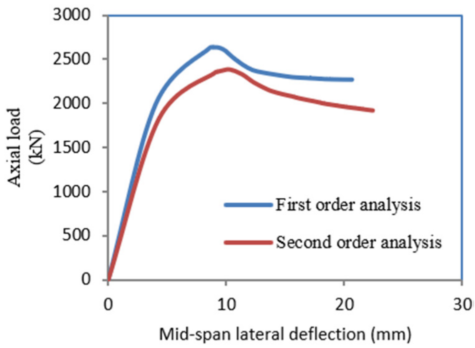


Fig. 5. Load-deflection relationships of Model 2 ($\rho$ = 0.014).

Neglecting the *p-δ* effects, the load capacity is 2635 kN, whereas it is 2383 kN when considering them. Therefore, the reduction in the axial load is 9.57%, which is much greater than 5%. Through the property module in Abaqus, the area of the cross-section of the longitudinal bars was changed and the reinforcement ratio was increased to 0.045. Then, the analyses were repeated and Figure 6 shows the load-deflection relationships. The secondary moment reduced the load capacity from 3630.76 to 3336 kN, a decrease of 8.1%. This suggests that increasing the reinforcement ratio for a slender column reduces the effects of the secondary moments, but the column remains in its state as a slender column. Again, this result confirms the reliability of defining the slenderness ratio of the RC columns depending on their geometry without taking the reinforcement area into account, as in the ACI Code.

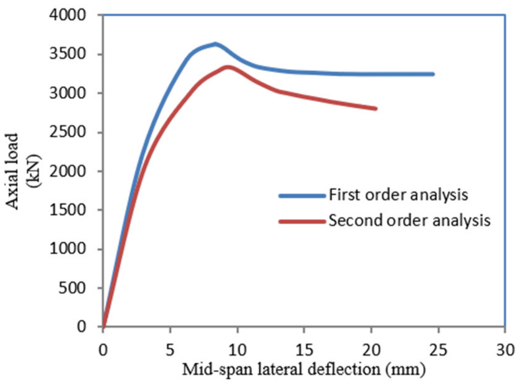


Fig. 6. Load-deflection relationships of Model 2 ($\rho$ = 0.045).

## IV. NON-PRISMATIC MODELS

Three RC non-prismatic columns were simulated under the effect of eccentric loads. The column models were pin-ended with a single eccentricity of 100 mm at the larger end. The three columns were tapered from 400×400 mm at the top to 200×200 mm at the bottom. The longitudinal steel rebars were parallel to the inclined edges of the columns. The reinforcement ratio calculated based on the mid-span cross-section area (area of the average cross-section) was 0.014. The transverse reinforcement was Ø 10 mm at 200 mm stirrups. Table I demonstrates other details of the models. The slenderness ratios were computed based on the average cross-sections.

TABLE I. PROPERTIES OF NON-PRISMATIC MODELS

| Model number | Length (mm) | Slenderness ratio |
|---|---|---|
| 3 | 2700 | 30 |
| 4 | 3060 | 34 |
| 5 | 3420 | 38 |

### A. *Model 3*

The slenderness ratio of Model 3 was 30 with a zero value of $M_1$. Therefore, its slenderness ratio is less than the limit of 34 given by (1).

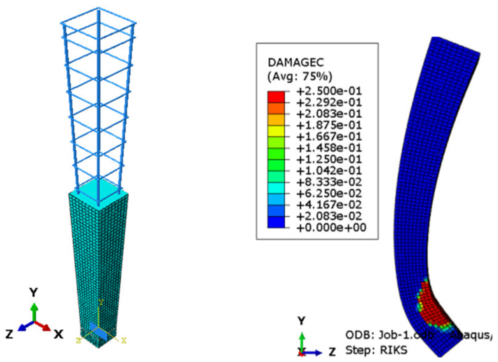


(a) (b)

Fig. 7. (a) View cut of meshed Model 3, (b) Failure mode of Model 3.

Figure 7 provides the view cut of the meshed model and its failure mode. The failure mode is the crushing of the concrete at a point close to the smaller end. Figure 8 theiscloses results of the first and second-order analyses. The failure load value given by the static Riks solution for the first-order analysis was 1536.5 kN. On the other hand, the second-order analysis gave a failure load of 1496 kN. , tA a resulthe reduction in the axial load capacity due to the effects of the secondary moment is 2.6%, which is less than 5%.

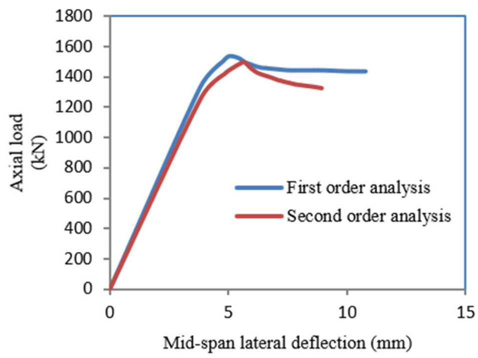


Fig. 8. Load-deflection relationships of Model 3.

### B. *Model 4*

The slenderness ratio of Model 4 was chosen as 34 to be the same as the limit value dividing the RC columns into short and long. The effects of the secondary moment in such a column are expected to cause a reduction in the axial load capacity of about 5%. Figure 9 showcases the results of the first- and second-order analyses. The axial load capacity given by the nonlinear first-order analysis was 1564 kN, whereas, when the $p$-$\delta$ effects were considered, the numerical result for the axial failure load was 1477.8 kN, indicating a reduction of 5.5%. This is close to the 5% reduction used as a criterion by the ACI Code to describe an RC column as short or slender.

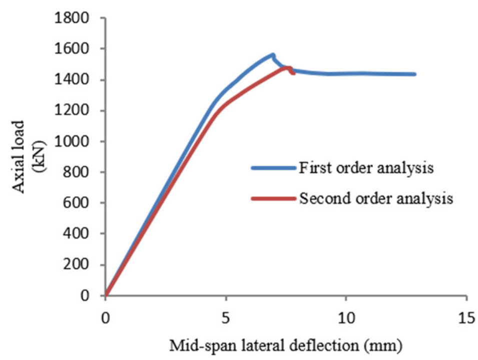


Fig. 9. Load-deflection relationships of Model 4.

### C. *Model 5*

The slenderness ratio of Model 5, based on the average cross-section, was chosen to be slender if it is a prismatic column having the average cross-section. When the geometric nonlinearity was ignored, the load capacity was 1586.4 kN, while it was reduced to 1491 kN due to the effects of the secondary moment. Thus, the reduction in load capacity was 6%, which is greater than the 5% reduction value adopted by the ACI Code. The Abaqus results evaluated well the slenderness ratio of the model based on the mid-span cross-section. Figure 10 portrays the load-deflection relationships.

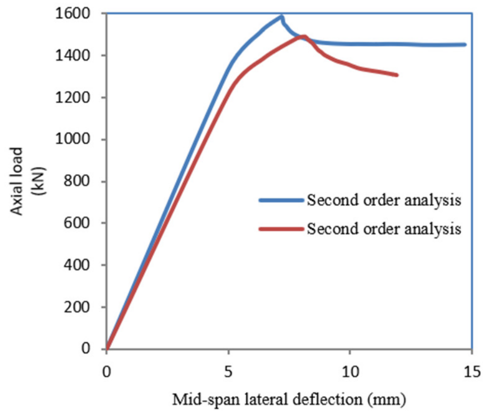


Fig. 10. Load-deflection relationships of Model 5.

Figure 11 exhibits the failure mode and stresses in the steel reinforcement of Model 5. The failure mode of Model 5, as well as other non-prismatic models, agrees with that expected for the loading case that concrete will be crushed at some distance from the smaller end. The shifting of the crushing location from the smaller end to a relatively larger cross-section somewhere close to it is caused by the existence of the eccentricity. The eccentricity varies from 100 mm at the larger end (top end) to zero at the bottom end. Therefore, the case of pure axial loading at the smaller end cross-section makes it stronger than the cross-section where the crushing occurs. Yielding of longitudinal bars located on the concave side is also expected due to the combined effect of axial and flexural loads, as both effects cause compressive stresses on the concave side.

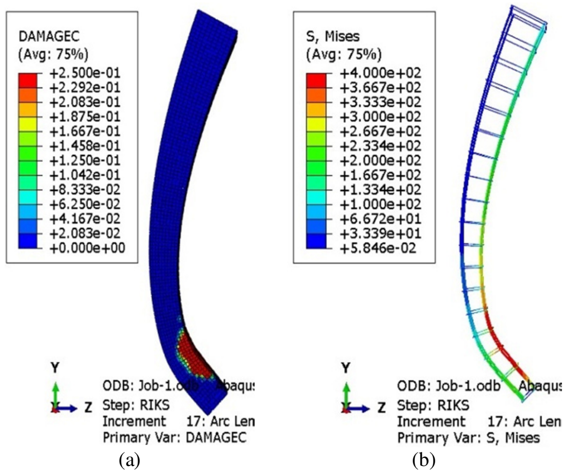


Fig. 11. Model 5: (a) failure mode, (b): reinforcement stresses.

Figure 12 displays the pattern of tensile cracks. As expected, the location of the crack is on the convex side of the column opposite the location of the crushing cracks.

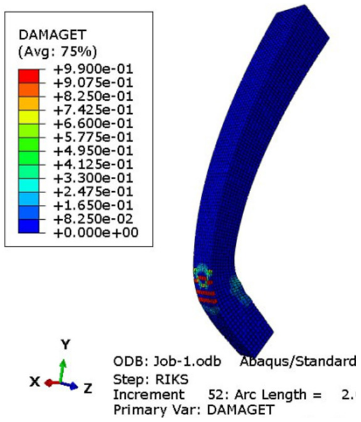


Fig. 12. Tensile cracks in Model 5.

## V. CONCLUSIONS

Based on the Abaqus results, the following conclusions can be obtained:

- The effects of the secondary moments in the prismatic columns agree with the ACI Code limitations. The reduction in load capacity is less than 5% in short columns and greater than 5% in slender columns.
- For slender RC prismatic and non-prismatic columns, the effect of the secondary moment on the load-deflection relationship appears in an early stage. This reveals the effect of the relatively large deformations that result in affective secondary moments in the early stages of loading.
- Using a reinforcement ratio of 0.014, which is close to the minimum limit of 0.01 that the ACI Code specifies for RC columns, keeps the effect of secondary moments lower than 5%. This indicates that a short column remains short even when a minimum reinforcement is provided, which in turn confirms the reliability of defining the slenderness ratio of RC columns depending on their geometry regardless of the amount of reinforcement.
- When the longitudinal reinforcement ratio increased from 0.014 to 0.045, the effect of the secondary moment was reduced from 9.57% to 8.1%. Thus, increasing the reinforcement ratio of an RC slender column reduces the effects of the secondary moments but does not change the column to a short one. Again, this finding agrees with the fact that the codes define the slenderness ratio of RC columns depending on their dimensions regardless of the amount of reinforcement.
- Under the effect of an eccentric axial load, the tapered column will not fail at the smaller cross-section but at some distance from it, due to the combined axial and flexural effects.
- For the evaluation of the slenderness ratio, an RC column that is linearly tapered can be considered as a prismatic column having a cross-section equal to its average cross-section. In other words, the ACI Code formulae regarding slenderness are applicable for tapered columns depending

on their average cross-section for the evaluation of the radius of gyration of the cross-sectional area.

## REFERENCES


[1] C. G. Chiorean, D. Passera, R. Ferrari, and E. Rizzi, "An implementation for 2nd-order M-N coupling and geometric stiffness adaptation in tapered beam-column elements," *Engineering Structures*, vol. 225, Dec. 2020, Art. no. 111241, https://doi.org/10.1016/j.engstruct.2020.111241.

[2] M. H. Saraçaoğlu and S. Uzun, "Stability analysis of columns with variable cross-sections," *Journal of Structural Engineering & Applied Mechanics*, vol. 3, no. 3, pp. 169–179, Sep. 2020, https://doi.org/10.31462/jseam.2020.03169179.

[3] A. Alkloub, R. Allouzi, and H. Naghawi, "Numerical Nonlinear Buckling Analysis of Tapered Slender Reinforced Concrete Columns," *International Journal of Civil Engineering*, vol. 17, no. 8, pp. 1227–1240, Aug. 2019, https://doi.org/10.1007/s40999-019-00395-5.

[4] P. K. Mehta and P. J. M. Monteiro, *Concrete: Microstructure, Properties, and Materials*, 4th ed. McGraw-Hill Education, 2014.

[5] N. F. A. Brant, "Reinforced concrete columns of variable cross section," Ph.D. dissertation, City University London, 1984.

[6] M. C. Head and J. D. Aristizabal-Ochoa, "Analysis of Prismatic and Linearly Tapered Reinforced Concrete Columns," *Journal of Structural Engineering*, vol. 113, no. 3, pp. 575–589, Mar. 1987, https://doi.org/10.1061/(ASCE)0733-9445(1987)113:3(575).

[7] R. Pedreschi, "A preliminary study of the strength of non-prismatic columns using fabric formwork," in *Proceedings of IASS Annual Symposia*, Amsterdam, Netherlands, Aug. 2015, vol. 2015, pp. 1–12.

[8] M. H. Saraçaoğlu and S. Uzun, "Stability analysis of columns with variable cross-sections," *Journal of Structural Engineering & Applied Mechanics*, vol. 3, no. 3, pp. 169–179, Sep. 2020, https://doi.org/10.31462/jseam.2020.03169179.

[9] M. Zahid and S. Al-Zaidee, "Validated Finite Element Modeling of Lightweight Concrete Floors Stiffened and Strengthened with FRP," *Engineering, Technology & Applied Science Research*, vol. 13, no. 4, pp. 11387–11392, Aug. 2023, https://doi.org/10.48084/etasr.6055.

[10] J. A. Kadhim and S. R. A. Zaidee, "Validated three-dimensional finite element modeling for static behavior of RC tapered columns," *Journal of the Mechanical Behavior of Materials*, vol. 32, no. 1, Jan. 2023, https://doi.org/10.1515/jmbm-2022-0226.

[11] P. C. Nguyen, D. D. Pham, T. T. Tran, and T. Nghia-Nguyen, "Modified Numerical Modeling of Axially Loaded Concrete-Filled Steel Circular-Tube Columns," *Engineering, Technology & Applied Science Research*, vol. 11, no. 3, pp. 7094–7099, Jun. 2021, https://doi.org/10.48084/etasr.4157.

[12] J. Wight, *Reinforced Concrete: Mechanics and Design*, 7th ed. Hoboken, NJ, USA: Pearson, 2015.

[13] J. M. de Araújo, "Comparative study of the simplified methods of Eurocode 2 for second order analysis of slender reinforced concrete columns," *Journal of Building Engineering*, vol. 14, pp. 55–60, Nov. 2017, https://doi.org/10.1016/j.jobe.2017.10.003.

[14] P. Frost Perez, "Second order effects in RC columns: comparative analysis of design approaches," M.S. Thesis, Gent University, Belgium, 2010.

[15] L. Hamzaoui and T. Bouzid, "The Proposition of an EI Equation of Square and L–Shaped Slender Reinforced Concrete Columns under Combined Loading," *Engineering, Technology & Applied Science Research*, vol. 11, no. 3, pp. 7100–7106, Jun. 2021, https://doi.org/10.48084/etasr.4048.

[16] M. Hafezolghorani, F. Hejazi, R. Vaghei, M. S. B. Jaafar, and K. Karimzade, "Simplified Damage Plasticity Model for Concrete," *Structural Engineering International*, vol. 27, no. 1, pp. 68–78, Feb. 2017, https://doi.org/10.2749/101686616X1081.

[17] *Building Code Requirements for Structural Concrete and Commentary*, ACI 318-19, American Concrete Institure, 2019.